THE EFFECTIVENESS OF A GASEOUS FILM ON A TUBULAR SURFACE

E. P. Volchkov and V. Ya. Levchenko

Zhurnal Prikladnoi Mekhaniki i Tekhnicheskoi Fiziki, No. 1, pp. 115-120, 1966

ABSTRACT: A number of articles on protecting structural elements from high-temperature gas flows deal with the effectiveness of gaseous films and various methods for producing such films [1-9]. All these investigations were carried out for smooth surfaces. In technology, however, we often encounter the need for cooling surfaces with large-scale roughness.
This article is devoted to an experimental study of protective cooling of surfaces with regular macroroughness commensurable with the thickness of the boundary layer.

1. A diagram of the experimental set-up is given in Fig. 1. After the stream of air leaves the blower 1, it is divided into two parts. The main part of the air 2 enters the working section 5 after passing through an electric heater 4 in which the air is heated to 55-100° C. The other part of the air, at room temperature, is employed as the protective film on the wall. The working section of the set-up is a channel with rectangular cross section (Figs. 2 and 3) 150 mm wide. The lower wall of the working section served as a test panel. It was demountable, which made it possible to study different methods for producing the film.

Most of the experiments were conducted by delivering secondary air to the working section through a slit parallel to the main flow and the wall (Fig. 2). The height of the slit s was varied by shifting the test panel.

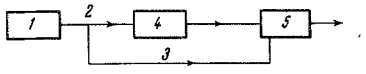

Fig. 1

The partition separating the hot and cold flows at the inlet to the working section was made of textolite. The tubular experimental panel was composed of hard rubber elements. In order to ascertain the influence of macroroughness on the effectiveness of the film, it was necessary to acquire data for a smooth surface. Since the experimental data of different authors on film cooling of smooth surfaces differ considerably (refer, for example, to [3]), which is explained by the conditions under which the experiments were conducted, we conducted special tests with a smooth panel made of a textolite plate 15 mm thick.

The velocity and temperature profiles were measured at the inlet to the working section, also at various points along its length in the course of the experiments. The velocities were measured by means of a Pitot tube having a diameter of 0.5 mm connected with a static pressure tube. An MMN type micromanometer was the indicating instrument. The temperature field was measured with a nichrome-constantan thermocouple made of 0.1 mm wire. The thermocouple was stretched on a textolite fork and placed in a horizontal plane across the flow. This arrangement of the thermocouple practically excluded errors in measuring temperatures due to radiation and heat losses along the wires. The voltage of the thermocouple was measured by a type P-2-1 potentiometer. In a number of experiments, we measured the temperature of the test panel with the aid of chromel-copel thermocouples caulked at several points along their lengths.

Typical velocity and temperature profiles at the inlet to the working section (x = 0) are presented in Fig. 4. Heat exchange through the partition separating the main and secondary air flows leads to some distortion of the initial temperature profile. This situation can affect only the initial section of the stream x_0, and the value at x_0 was excluded in processing experimental data.

Figure 4 also shows a typical temperature profile (b) in the zone where the main flow mixes with the stream along the wall (x > 0). The nature of the profile provides evidence of the absence of heat losses at the wall. The wall temperature determined from the profile practically coincided with the directly measured temperature of the surface with $t_w \leqslant 50°$ C. At higher wall temperatures, the adiabatic temperature profile of the gas was distorted at the wall due to noticeable heat conduction, and the thermocouples in the panel showed a lowered value of the temperature as compared with the adiabatic. The temperature obtained by extrapolating the section of the gas temperature profile at the wall which was not distorted by heat conduction was taken to be the wall temperature.

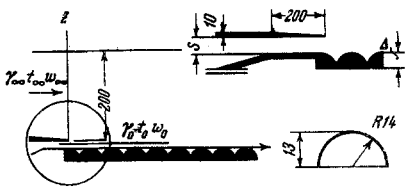

Fig. 2

The average velocity w_0 was determined by integrating the velocity profile in the slit; the velocity outside the boundary layer was taken as the velocity w_∞ of the main flow. By integrating the velocity profile at the inlet of the main flow to the working section, we determined the initial momentum thickness

$$\delta_{00}^{**} = \int_s^\infty \frac{\gamma w}{\gamma_\infty w_\infty}\left(1 - \frac{w}{w_\infty}\right) dz,$$

which was used to calculate the length of the effective initial hydrodynamic section L ≈ 0.65 m. The measured degree of turbulence of the main flow $\langle |w_\infty'| \rangle / w_\infty$ was equal to 2.5%.

2. The principal regime parameters of the experiments on slit cooling of smooth and tubular surfaces are presented in Table 1.

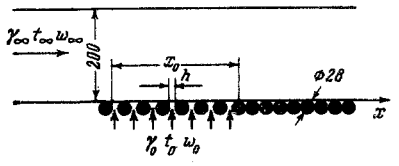

Fig. 3

The principal parameter characterizing the intensity of mixing of the gaseous film with the main flow and its protective properties is the dimensionless adiabatic wall temperature or the "effectiveness" $\theta = (t_\infty - t_{aw}) / (t_\infty - t_0)$. The results of the experiments on a smooth surface with $m = \gamma_0 w_0 / \gamma_\infty w_\infty < 1$ are given in Fig. 5. The continuous curve shows the results from the theoretical formula [1]

$$\theta = (1 + 0.24\xi)^{-0.8}$$

$$\left(\xi = \frac{\Delta x}{ms} R_s^{-0.25}, \quad R_s = \frac{\gamma_0 w_0 s}{\mu_\infty}, \quad \Delta x = x - x_0\right). \qquad (2.1)$$

Here R is the Reynolds number, μ the viscosity of the main flow, and x_0 the length of the initial section of the stream adjacent to the wall, for which θ = 1.

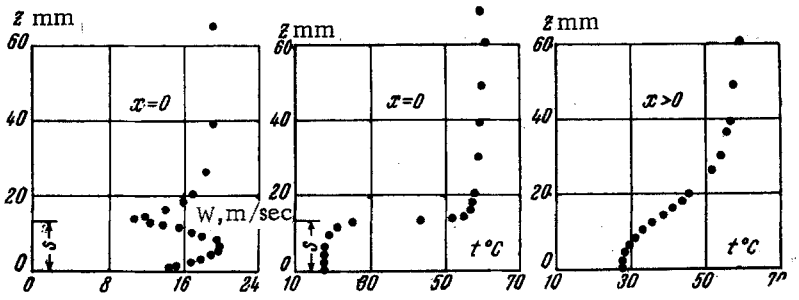

Fig. 4

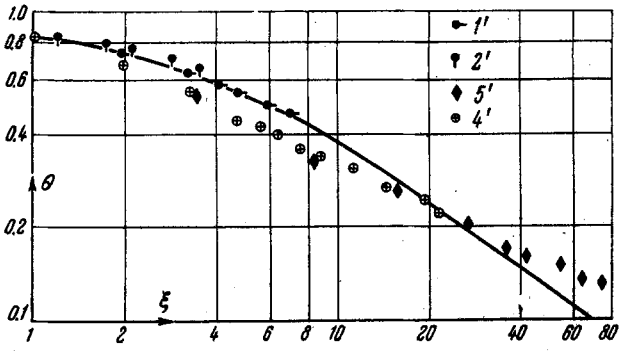

Fig. 5

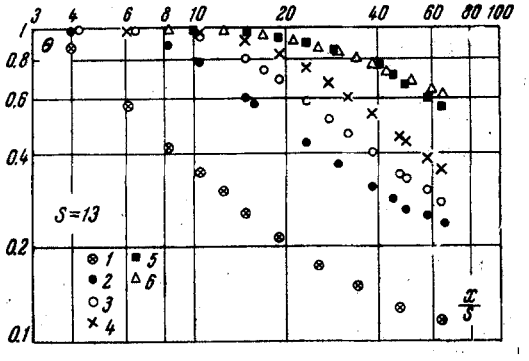

Fig. 6

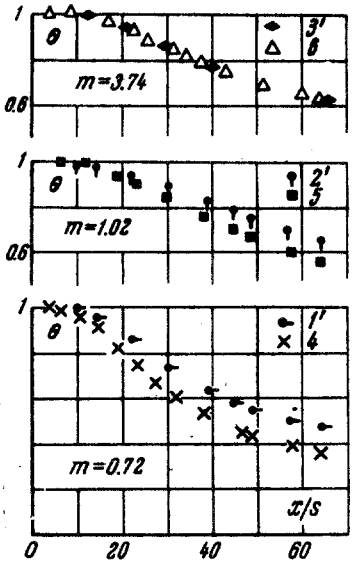

Fig. 7

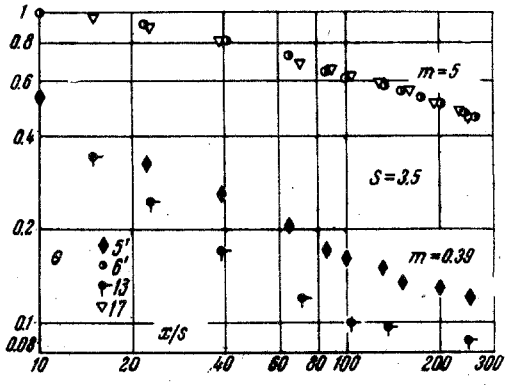

Fig. 8

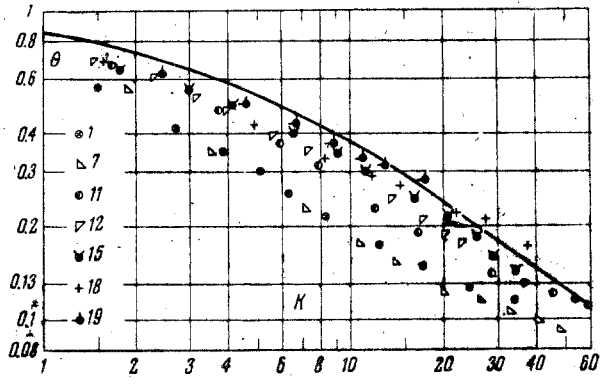

Fig. 9

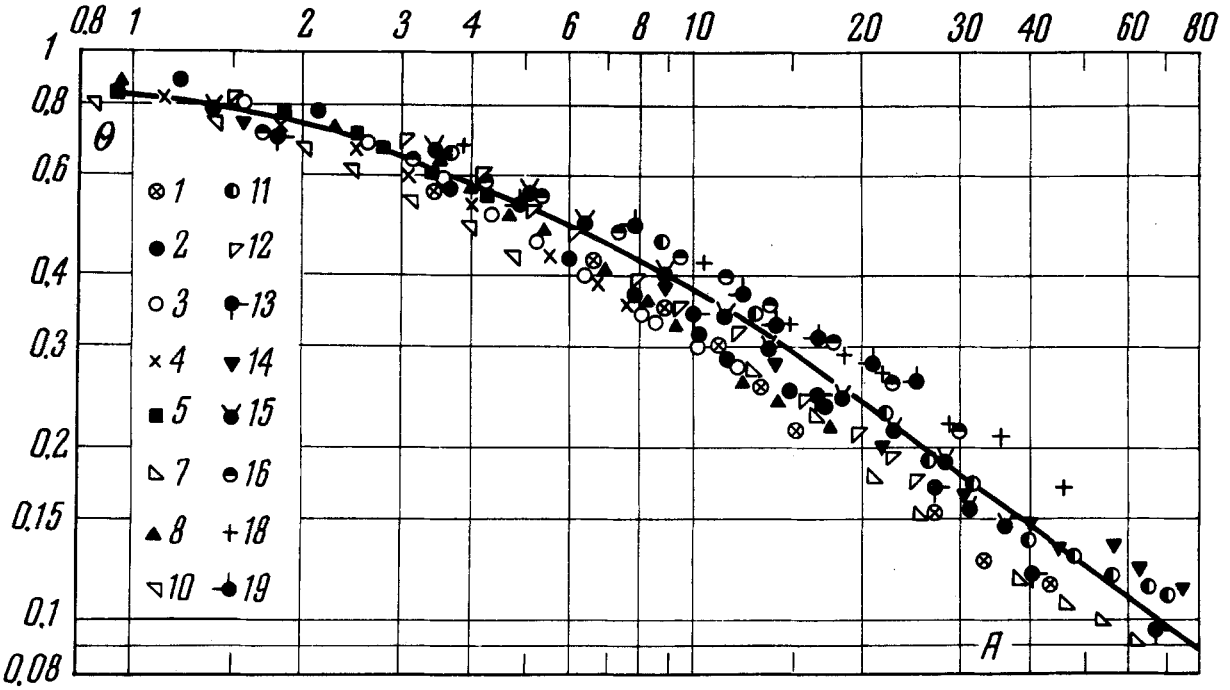
0.8
1
2
3
4
6
8
10
20
30
40
60
80
1
0.8
0.6
0.4
0.3
0.2
0.15
0.1
0.08
θ
1
2
3
4
5
7
8
10
11
12
13
14
15
16
18
19
A

Fig. 10

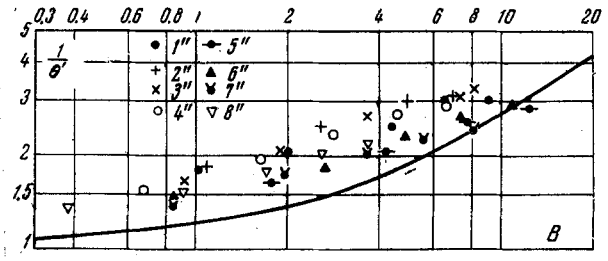
0.3
0.4
0.6
0.8
1
2
4
6
8
10
20
5
4
3
2
1.5
1
1/θ'
1″
2″
3″
4″
5″
6″
7″
8″
B

Fig. 11

Figure 6 shows typical curves of change in θ with length for different values of the injection parameter m and a fixed slit height in the experiments with a tubular panel. Figure 7 gives a comparison of the results from experiments with tubular and smooth surfaces conducted with the same slit height s = 13 mm ($s/\Delta = 1$) for approximately identical regimes. As can be seen here, when $m < 1$, there is a noticeable difference in the distribution of the "effectiveness" θ over the length; however, this difference is smoothed out as the injection parameter increases and vanishes completely at sufficiently large m. It is interesting that the same pattern is also observed at small relative values of s (Fig. 8). Apparently, when flows move at low velocities over a tubular wall, the streamlines are of a wavelike nature and the "effective wettability" of the surface is increased as compared with a smooth surface. In addition, waviness of the motion leads to more intense mixing of the film with the main flow. At high flow velocities, the intense vortex between tubes creates a unique air cushion and the stream adjacent to the wall is propagated along a fictitious smooth surface formed by the tops of the tubes and the vortex between the tubes. In the experiments described here, the velocity of the gas near the surface is determined by the parameter m.

The nature of the change in θ with length indicates that the process of mixing of the gas film with the main flow near a tubular surface obeys (to a considerable extent) the same laws as the process of mixing near a smooth surface. In accordance with this, the experimental data on the "effectiveness" should be processed as a function of the parameter ξ [refer to formula (2.1)] corrected by some factor which takes account of the change in the "effective wettability" of the surface with changes in the flow velocity. Figure 9 shows the "effectiveness" as a function of this parameter.

Table 1

Points	s, mm	w_∞, m/sec	w_0, m/sec	m	$\frac{R_s}{10^3}$
		Smooth panel			
1′	13	19.2	11.8	0.71	9
2′	13	19.3	17.1	1.02	13.1
3′	13	13.2	43.2	3.76	32.8
4′	6.5	20.5	13.2	0.74	5.1
5′	3.5	20.4	6.8	0.38	1.4
6′	3.5	8	29.6	5	6
		Tubular panel			
1	13	21.5	4.5	0.23	3.5
2	13	21.7	8.6	0.45	6.7
3	13	19	9.5	0.57	7.4
4	13	19.3	12.2	0.73	9.5
5	13	19.1	17.1	1.03	13.4
6	13	13.8	43.8	3.72	33
7	10	21.4	4.3	0.23	2.6
8	10	19.3	8.8	0.53	5.4
9	10	19.2	13.4	0.83	7.4
10	10	19	17.5	1.06	10.5
11	6.5	19.9	5.4	0.31	2.1
12	6.5	18.1	10.5	0.65	4.1
13	3.5	20.1	7	0.4	1.4
14	3.5	20.4	8.1	0.45	1.7
15	3.5	20.2	15.7	0.88	3.4
16	3.5	18.8	18.3	1.14	3.8
17	3.5	8.2	31.9	5.04	6
18	2	16.8	10.8	0.73	1.2
19	2	17.1	15.7	1.05	1.8

The magnitude of the initial section x_0 was found by extrapolation of the exponential law of variation of θ with the distance x/s from the point where $\theta = 1$ (Fig. 6). As can be seen, the parameter ξ collects the experimental points outside the dependence on slit height s (the ratio s/Δ); however, there is a noticeable divergence of the points plotted by the parameter m. The curve (2.1) for a smooth surface lies above the experimental points. One may also note that at great relative distances from the initial section, the values of the "effectiveness" on a tubular surface asymptotically approach the values of the "effectiveness" on a smooth surface.

In accordance with these peculiarities of variation in the dimensionless adiabatic temperature of a tubular wall, the factor [coefficient] associated with the parameter ξ should be equal to unity at high flow velocities (under the conditions of the experiments described above, this is equivalent to the correcting factor being equal to unity for large values of the injection parameter m) with sufficiently large values of Δx, very low values of Δx, and with tube height equal to zero. A function of the following type may serve as the first approximation to such factors:

$$\alpha_k = \left[1 + \frac{\Delta}{m\Delta x}\left(1 + \frac{\Delta}{m\Delta x}\right)^{-2}\right]^k. \qquad (2.2)$$

Table 2

Points	h, mm	w_∞, m/sec	w_0, m/sec
1″	8	25	1.29
2″	8	18.6	1.42
3″	8	14.1	1.78
4″	8	9.4	1.75
5″	4	9.4	1.35
6″	4	17	3.24
7″	4	9.8	3.24
8″	4	10.9	5.91

Figure 10 shows all the obtained experimental data on "effectiveness" θ on a tubular surface with $m \leqslant 1$ processed as a function of the parameter $A = \xi\alpha_4$. The continuous line represents calculations from the formula

$$\theta = (1 + 0.24\,A)^{-0.8}, \qquad (2.3)$$

which coincides with formula (2.1) for a smooth surface when $\Delta = 0$. Formula (2.3) describes the experimental data when $A \leqslant 70$ with accuracy to ±25%.

3. A series of experiments was conducted on a tubular surface with the film on the initial section between tubes (Fig. 3). The test panel was made of wood cylinders 28 mm in diameter. The gap h between tubes amounted to 4 and 8 mm in the initial section. The length of the initial section $x_0 = 210$ mm for h = 4 mm and $x_0 = 202$ mm for h = 8 mm.

This method of producing a film can be identified with creating a film through an initial porous section, which was studied in [9, 1]. In [1] a formula for calculating the "effectiveness" with critical and supercritical injection is given, which can be reduced to the form

$$\theta = \left[1 + 0.24\left(\frac{\mu_\infty}{q} R_{\Delta x}^{0.8}\right)^{1.25}\right]^{-0.8} \qquad \left(\theta = \frac{t_\infty - t_{aw}}{t_\infty - t_0}\right). \qquad (3.1)$$

Here μ_∞ is the dynamic viscosity coefficient of the main flow, q is the gas flowrate for the film per unit width of the surface. An analogous formula for subcritical injection is of the form

$$\theta' = \left[1 + 0.24\left(\theta_0 \frac{\mu_\infty}{q} R_{\Delta x}^{0.8}\right)^{1.25}\right]^{-0.8},$$

$$\theta' = \frac{t_\infty - t_{aw}}{t_\infty - t_{w0}}, \quad \theta_0 = \frac{t_\infty - t_{w0}}{t_\infty - t_0}, \quad R_{\Delta x} = \frac{\gamma_\infty w_\infty \Delta x}{\mu_\infty}. \qquad (3.2)$$

Here θ_0 is the dimensionless wall temperature at the end of the porous section.

The regime parameters of these experiments are presented in Table 2. The air injection velocity w_0 was calculated from the measured flowrate. In Fig. 11, the experimental data on the "effectiveness" θ' are processed as functions of the parameter

$$B = \left(\theta_0 \frac{\mu_\infty}{q} R_{\Delta x}^{0.8}\right)^{1.25}.$$

It can be seen that this parameter satisfactorily generalizes the experimental data (the dispersion of the experimental points does not exceed ±15%). The continuous line represents the calculations

from formula (3.2) for a smooth surface. There is a noticeable difference in the distribution of the "effectiveness" on tubular and smooth surfaces which, as in the case of jet cooling, is smoothed out with distance from the injection site, that is, as the boundary layer increases. Thus, the macroroughness influences the "effectiveness" through the ratio Δ/Δ_x. The limited scope of our investigations does not as yet permit determining the quantitative laws of this effect.

REFERENCES

1. S. S. Kutateladze and A. I. Leont'ev, "A thermal film on a turbulent gas boundary layer," Teplofizika vysokikh temperatur, vol. 1, no. 2, 1963.

2. V. Ya. Borodachev, A Theoretical and Experimental Investigation of Air Film Cooling of a Flat Plate [in Russian], Oborongiz, 1956.

3. Garnett, Eckert, and Birkebak "An analysis of the principal characteristics of a turbulent boundary layer for an air flow delivered through tangential slits," Transactions of the American Society of Mechanical Engineers, J. Heat Transfer, ser. C, vol. 83, no. 3, 1961.

4. Chin, Skirvin, Hayes, Barkgraf, "Film cooling with multislit and grid injection," Transactions of the American Society of Mechanical Engineers, J. Heat Transfer, ser. C, vol. 83, no. 3, 1961.

5. Seban, Beck, "Velocity and temperature profiles in a turbulent boundary layer with air delivered through a tangential slit," Transactions of the American Society of Mechanical Engineers, J. Heat Transfer, ser. C., vol. 84, no. 1, 1962.

6. R. A. Seban, "Heat transfer and effectiveness for a turbulent boundary layer with tangential fluid injection," Transactions of the ASME. J. Heat Transfer, ser. C, vol. 82, no. 4, 1960.

7. Sellers, "Combined external and internal cooling," AIAA Journal, vol. 1, no. 9, 1963.

8. Sellers, "Gaseous film cooling with multiple injection stations," AIAA Journal, vol. 1, no. 9, 1963.

9. Niishi Nishiwaki, Masaru Hirata, and Akira Tsuchida, "Heat transfer on a surface covered by a cold air film," Internat. Development in Heat Transfer, part IV, section A, 1961.

18 March 1964 Novosibirsk